The HKU Scholars Hub   The University of Hong Kong   香港大學學術庫

Title	**Color variation reduction of gan-based white light-emitting diodes via peak-wavelength stabilization**
Author(s)	**Chen, H; Tan, SC; Hui, SYR**
Citation	**IEEE Transactions on Power Electronics , 2014, v. 29 n. 7, p. 3709-3719**
Issued Date	**2014**
URL	**http://hdl.handle.net/10722/196278**
Rights	**IEEE Transactions on Power Electronics . Copyright © Institute of Electrical and Electronics Engineers.**

Color Variation Reduction of GaN-Based White Light-Emitting Diodes Via Peak-Wavelength Stabilization

Huan-Ting Chen, *Member, IEEE*, Siew-Chong Tan, *Senior Member, IEEE*, and S. Y. (Ron) Hui, *Fellow, IEEE*

Abstract—The color, electrical, and thermal properties of LED devices are highly dependent on one another. The peak wavelength of GaN-based white LED shifts in opposite directions under the influences of current and junction temperature change. This affects the correlated color temperature (CCT). Importantly, duty cycle control for LED dimming does not provide constant color (against conventional wisdom). An analysis model that links the peak wavelength, electrical, and thermal properties of LED devices is proposed. The color-shift trend of the LED with respect to the changes in its thermal and electrical operating conditions is described. The stabilized CCT performance of a dc or a bilevel-driven LED over a dimming range is found to be a result of the complex interactions between the selected current levels, duty cycle, thermal resistances of the heatsink and device, heat dissipation conversion ratio, and the physical parameters of the LED device. The predicted color variation is verified by experimental results, which demonstrate that the CCT stabilization of an LED with a dc drive requires less thermal energy than that with a bilevel drive. For a given thermal design, the reduction in CCT variation during light intensity change is possible via the combined adjustment of the current level and its duty cycle over the dimming operation.

Index Terms—Correlated color temperature (CCT), color control, light-emitting diode (LED), lighting system, n-level driving, white LED.

I. INTRODUCTION

DUE to its small size and long lifetime, the high-power light-emitting diode (LED) is considered an attractive candidate for replacing incandescent and fluorescent lightings for general energy-efficient illumination purpose. However, there are still some critical aspects requiring attention when it comes to applying LED for general lighting. The issue lies mainly on

the junction temperature of LED, which is an important parameter affecting the lifetime, efficiency, forward voltage drop, and spectral power distribution of the device, when it comes to designing a high-quality light source [1], [2].

When current flows through the LED, most of the electrical energy is converted into heat, which is accumulated at the device junction. An increasing current will generate more heat, which consequently reduces the quantum efficiency, thereby lowering the luminous efficacy of the LED and also shifting the spectrum of the emitted light. The light output of a packaged LED reaches a maximum level at a certain current density, and thereon decreases with an increasing current density. The relationship of the photometric, electrical, and thermal aspects of the LED have been described by a photo-electro-thermal (PET) theory for LED systems and applications [3], [4]. It has been demonstrated that operating the LED at its rated power does not necessarily guarantee an optimal luminous performance unless proper thermal design is considered [5].

Chromatically, the spectrum of a GaN-LED shifts toward shorter wavelengths (i.e., blue shift) with an increasing current. This is due to the piezoelectricity-induced quantum confined Stark effect [6]. On the contrary, there is red shift in the spectrum of the GaN-LED with an increasing temperature. This is attributable to the variation in the semiconductor bandgap due to the change in temperature [7]. Chromaticity shift that results from the change in the spectrum are affected by the change in amplitude, peak wavelength, and full-width-at-half-maximum parameter of the spectrum. In the case of RGB white LED systems, a change of less than 1% in amplitude or 1-nm shift in the peak wavelength of certain colored LEDs can result in a perceivable color change [8].

The color deviation of the emitted light of an LED is mainly attributed to the variation of the electrical and thermal stresses on the LED device. For multicolored LED systems, the color deviation can be compensated by feedback control using light spectrum/temperature detectors, color evaluation system, and circuit control [9]. For components made up of phosphors, their endurance property is the critical feature that diminishes any color variation resulting from an incident light photon. A high-and-stable light quality is demanded from the white LEDs in the domain of general lighting [1], [2].

To allow one to obtain high-color-quality light from the white LEDs, it is necessary to first understand the mechanisms that will affect the color deviation. It is known that the main reason for a shift of the spectrum (i.e., color variation) of an operating LED is due to the change of its junction temperature or

driving current. It is also known that the spectrum is also affected by its package materials (i.e., phosphor and silicon etc.), which degrade over their operating lifetime, leading to further deterioration of the spectrum consistency. For this reason, to achieve high color reliability in white LEDs, highly reliable materials for the packaging, such as phosphors, transparent silicon, blue chips, and reflectors, are developed. Furthermore, well-structured packages preventing heat accumulation in the phosphor materials of the LED device, which help in reducing color deviation, should be employed [10].

White LEDs driven by dc, pulsewidth-modulated (PWM) current, and bilevel current exhibit different color shift properties [11], [12]. This feature must be considered when it comes to designing a color-stable LED-based lighting system. Similar to other light sources used for general lighting, white LEDs have to satisfy the dimming needs of general illumination and concurrently conforming to the color-shift requirement. A noticeable color shift during dimming is generally unacceptable in some general lighting applications. With different dimming schemes, the spectrum and luminous efficacy change of the LEDs are different. For the InGaN-based blue, green, and pc-white LEDs, the peak wavelength shifts in opposing directions under the dc and PWM dimming schemes. In particular, with dc dimming, the peak wavelength shows a blue shift with increased light intensity (i.e., increased current level). This is attributed to the band filling and quantum-confined Stark effects [6]. With PWM dimming, InGaN LEDs exhibit a red shift with increased light intensity (i.e., increased duty cycle). This is dominantly caused by the increase in junction heat [10].

A thermal management approach for minimizing the color shift of white LEDs under dc, PWM, and bilevel drive, through the design of the heatsink, has been proposed in [12]. The theoretical aspects and impact of the n-level driving technique, which includes bilevel driving, on the color-shift and luminous efficacy properties of white LEDs are discussed through a mathematical model [13]. Stationary and adaptive color-shift reduction methods are proposed based on this model [14]. However, worth noting is that the works presented in [12]–[14] are based on a simplistic thermal model of the LEDs which does not reflect the true luminous and color properties of the LED, as will be explained later in this paper.

Chromaticity values are commonly used for characterizing the color appearance of a light source. Parameters commonly used for quantifying perceivable color difference are the color temperature and the chromaticity coordinates. In LED driving, most literatures have been focused on how the variations of these parameters are minimized when dimmed to achieve high-quality lighting. Few have investigated the change of the peak wavelength of LED under electrical and thermal stresses.

In this paper, a report describing the actual behavior of the peak wavelength of white LEDs during dimming and a realistic mathematical model linking the complex relationships between the peak wavelength, the drive current, and the junction temperature over dimming are presented. In addition, a systematic method for minimizing CCT variation in an LED system under various driving schemes is proposed. Experimental results are provided to validate the model and the proposed design.

II. PEAK-WAVELENGTH MODELING WITH CONSIDERATION TO THE THERMAL AND ELECTRICAL FACTORS

Light emission of LEDs is the result of the spontaneous recombination of electron–hole pairs at the junction of the LED which simultaneously releases photons. Based on the donor–acceptor pair composition theory [15], the transitional photon energy can be expressed as

$$hv_p = h\frac{C}{\lambda_p} = (E_g - E_D + E_A) + \frac{e^2}{4\pi\varepsilon R\varepsilon_0} \quad (1)$$

where h is the Planck constant, v_p is the peak frequency, c is the speed of light, λ_p is the peak wavelength, E_g is the bandgap energy, E_D and E_A are, respectively, the binding energy of the donor and acceptor, e is the elementary charge, ε is the dielectric constant, R is the distance of the donor–acceptor pair, and ε_0 is the vacuum dielectric constant. Thus, the emission peak wavelength of LEDs can be designed by the proper choice of the semiconductor material with an appropriate bandgap energy.

The energy of photons emitted from a semiconductor is given by its bandgap energy E_g. In an ideal diode, every electron injected into the active region will generate a photon. Law of energy conservation indicates that the injected electron energy (eV) is equal to the photon energy (hv_p), such that

$$eV = hv_p = (E_g - E_D + E_A) + \frac{e^2}{4\pi\varepsilon R\varepsilon_0} \quad (2)$$

where V is the forward voltage applied to the LED. The energy of an injected electron is converted into photon energy and is dependent on the process of electron–hole recombination. There are, however, several mechanisms which will cause the actual forward voltage of the LED to be slightly different from that extractable from theory. Firstly, an LED is not an ideal device and it contains a series resistance R_s resulting from the contact resistance and bulk resistance, which will contribute as a voltage drop of IR_s on the device when current I flows through the LED. Secondly, during the electron–hole injection process, the energy ΔE_{el} of electron and hole into the quantum well may be lost. The energy loss ΔE_{el} due to nonadiabatic injection of carriers is relevant in semiconductors with large band discontinuities [15]. The voltage drop ΔV_{el} due to energy loss ΔE_{el} can be expressed as $\Delta V_{el} = \Delta E_{el}/e$. Therefore, the total voltage drop across an LED is given by

$$V = \frac{E_g}{e} + IR_s + \Delta V_{el} \quad (3)$$

where the first term on the right-hand side of the equation (i.e., $\frac{E_g}{e}$) is the theoretically calculated forward voltage, the second term (i.e., IR_s) is the voltage drop due to the series resistance of the device, and the third term (i.e., ΔV_{el}) is the voltage drop due to the energy loss of nonadiabatic injection of carriers into the active region.

On the other hand, the Shockley equation describes the theoretical electrical property of a p-n junction as

$$I = I_s \exp\left(\frac{eV}{nkT_j}\right) \quad (4)$$

where I_S is the reverse saturation current, k is the Boltzmann constant, T_j is the absolute temperature of the junction, and n is the ideality factor of the diode [16], [17]. For a perfect diode, the ideality factor is 1.0. The ideality factor of most GaN-LED is more than 2 [18]. The high ideality factor of GaN-LED is attributed to tunneling and the influence of rectifying hetero-junctions and metal–semiconductor junctions that are present in heterostructure diodes. The I–V characteristic based on the Shockley equation requires modification to account the series resistance R_s. Hence, a more accurate electrical model of the LED can be given by

$$I = I_s \exp\left[\frac{e(V - IR_s)}{nkT_j}\right] \tag{5}$$

where the reverse saturation current is given by

$$I_s = eA \exp\left[\sqrt{\frac{D_p}{\tau_p}}\frac{n_i^2}{N_D} + \sqrt{\frac{D_n}{\tau_n}}\frac{n_i^2}{N_A}\right] = \beta T_j^2 \exp\left(-\frac{eV_0}{kT_j}\right). \tag{6}$$

Here, D_n and D_p are, respectively, the electron and hole diffusion constants, τ_n and τ_p are, respectively, the electron and hole minority-carrier lifetimes, N_A and N_D are, respectively, the acceptor and donor concentrations, n_i is the intrinsic carrier concentration, β is a constant parameter determined by the impurity concentration and junction area, V_0 is the potential difference between the bottom of the conduction band and the top of the valence band at a temperature of 0 K.

By combining (5) and (6),

$$I = \beta T_j^2 \exp\left(-\frac{eV_0}{kT_j}\right) \exp\left[\frac{e(V - IR_s)}{nkT_j}\right]. \tag{7}$$

The rearrangement of (7) with V as the subject of the function gives

$$V = nV_0 + \frac{nkT_j}{e}\ln\left(\frac{I}{\beta}\right) - \frac{2nkT_j}{e}\ln(T_j) + IR_s. \tag{8}$$

By substituting (8) into (3), the bandgap energy can be expressed as

$$E_g = enV_0 + \ln\left(\frac{I}{\beta}\right)nkT_j - \ln(T_j)2nkT_j - e\Delta V_{el}. \tag{9}$$

Next, by substituting (1) into (9), the peak wavelength λ_p and peak frequency ν_p can be obtained as

$$\frac{c}{\lambda_p} = v_p = \frac{enV_0}{h} + \ln\left(\frac{I}{\beta}\right)\frac{nkT_j}{h} - \ln(T_j)\frac{2nkT_j}{h} - \frac{e\Delta V_{el}}{h}. \tag{10}$$

Equation (10) relates the peak wavelength λ_p and peak frequency ν_p to the injection current (I) and junction temperature (T_j). Differentiating (10) with respect to T_j gives

$$\frac{d(v_p)}{d(T_j)} = \frac{en}{h}\frac{dV_0}{dT_j} + \ln\left(\frac{I}{\beta}\right)\frac{nk}{h} - \frac{2nk}{h}[\ln(T_j) - 1] - \frac{e}{h}\frac{d\Delta V_{el}}{dT_j}. \tag{11}$$

It is noted that the first and the fourth terms of the right-hand side of (11) (i.e., $\frac{en}{h}\frac{dV_0}{dT_j}$ and $\frac{e}{h}\frac{d\Delta V_{el}}{dT_j}$, respectively) can be ignored. Since V_o is a constant, dV_o/dt is zero. The $d\Delta V_{el}/dt$ is a second-order derivative which is negligible. Hence, with

consideration that the junction temperature is a function of the ambient temperature T_a and the associated physical parameters of the LED and its heatsink [3], (11) can be simplified into

$$\frac{d(\nu_p)}{d(T_j)} = \frac{d\left(\frac{c}{\lambda_p}\right)}{d(T_j)}$$

$$= \ln\left(\frac{I}{\beta}\right)\frac{nk}{h} - \frac{2nk}{h}[\ln(T_j) - 1]$$

$$= \ln\left(\frac{I}{\beta}\right)\frac{nk}{h}$$

$$- \frac{2nk}{h}\{\ln[T_a + (R_{jc} + NR_{hs})k_h IV] - 1\}. \tag{12}$$

As shown in (12), the peak frequency–temperature sensitivity is related to the injection current I, the heat dissipation coefficient k_h, and the thermal resistances of the LED device R_{jc} and its heatsink R_{hs}. Several important observations are drawn from (12) and are given as follows:

1) For the same injection current, the peak frequency–temperature sensitivity is higher with a lower heatsink thermal resistance. If a larger heatsink (i.e., lower R_{hs}) is used, the smaller the shift of the peak wavelength becomes.

2) For the same heatsink, the peak frequency is less sensitive to temperature variation at a lower current.

3) It has been shown in [13] that with the same heatsink and average injection current, driving the LED with a dc current gives a higher light output (i.e., high light efficiency) than that with a bilevel current [13], [19]. This means that k_h of LED with a dc driver is lower than that with the bilevel driver. Taking this into consideration, it can be deduced from (12) that the peak wavelength–temperature sensitivity of an LED with a dc driver is lower than that with a bilevel driver.

At a constant current, (10) can be expressed as

$$\frac{c}{\lambda_p} = \frac{nk}{h}\left[\frac{eV_0}{k} + \ln\left(\frac{I}{\beta}\right)T_j - \ln(T_j)2T_j - \frac{e\Delta V_{el}}{k}\right]$$

$$= \frac{nk}{h}\{a + T_j[b - 2\ln(T_j)]\}. \tag{13}$$

As will be illustrated with practical measurements, a is a positive coefficient and $a > |T_j[b–2\ln(T_j)]|$ and $b < 2\ln(T_j)$. Thus, $T_j[b–2\ln(T_j)]$ is a negative term. This suggests that the peak wavelength λ_p increases with increasing junction temperature at a constant current. As shown in Fig. 1, the calculated [using (13)] and experimentally measured peak wavelength versus the junction temperature is in good agreement with the explanation given previously.

The samples under test were mounted to a Peltier-cooled fixture, which was attached to an integrating sphere in accordance with the recommendations of International Commission on Illumination. The Peltier-cooled fixture was used to stabilize the LED's junction temperature for the optical measurements, and it is also used as an active temperature-controlled cold-plate for thermal measurements. Therefore, the Peltier-cooled fixture can
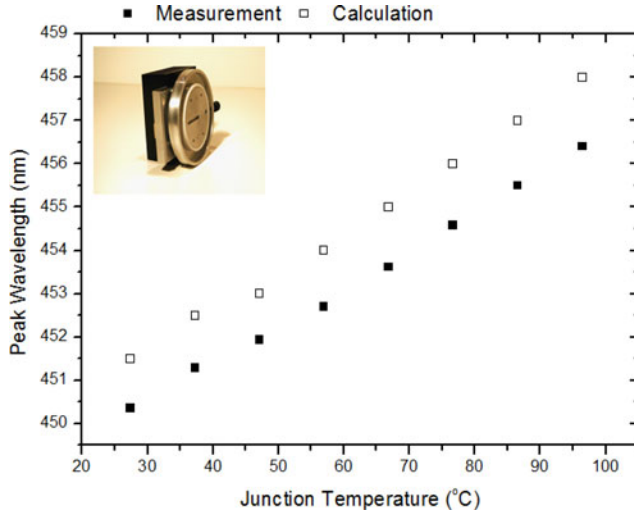
Fig. 1. Measured and calculated peak wavelength versus junction temperature of the sharp LED (GW5BWF15L00) at a constant current of 240 mA.

Fig. 2. Measured and calculated peak wavelength versus current of the sharp LED (W5BWF15L00) at a constant junction temperature of 56 °C.

be treated as a temperature-controlled heatsink, as shown in the picture given in Fig. 1.

The optical measurements of the LED samples were performed under steady-state thermal and electrical conditions using the TeraLED system. Once all the optical measurements were performed, the LED was switched OFF and the cooling transient of the LED package was monitored using the transient thermal tester (T3Ster) [20], [21]. The theoretical framework of evaluation of T3Ster was based on the distribution RC networks. The T3ster captures the thermal transient response in real time, records the cooling/heating curve, and then evaluates the cooling/heating curve so as to derive the thermal characteristics. Apart from the thermal and optical measurements, all temperature-dependent parameters of the LED (such as optical power, luminous flux, chromaticity coordinates, CCT, etc.) were measured and recorded. A 5-mA current was applied in the temperature range of 25–55 °C at incremental steps of 10 °C for the calibration of the temperature-sensitive parameters. The light output and transient thermal curves were measured only after 20 min of driving the LED while the heatsink temperature was being kept constant.

At a constant junction temperature, (10) can be expressed as

$$\nu_p = \frac{c}{\lambda_p} = \frac{nk}{h} \left[\frac{eV_0}{k} + \ln\left(\frac{I}{\beta}\right) T_j - \ln\left(T_j\right) 2T_j - \frac{e\Delta V_{\mathrm{el}}}{k} \right]$$
$$= \frac{nk}{h} \left[a' + b' \ln\left(\frac{I}{\beta}\right) \right]. \tag{14}$$

Notably, the peak wavelength decreases with an increasing current. This is also in good agreement with the calculated results [using (14)] and the experimental measurement, which are given in Fig. 2.

Equation (10) incorporates the spectral, electrical, and thermal aspects of the LED altogether. With the LED mounted onto the heatsink, its junction temperature is related to the injection current and the heatsink's thermal resistance. The first component $\left(\frac{enV_0}{h}\right)$ and the fourth component $\left(-\frac{en\Delta V_{\mathrm{el}}}{h}\right)$ on the
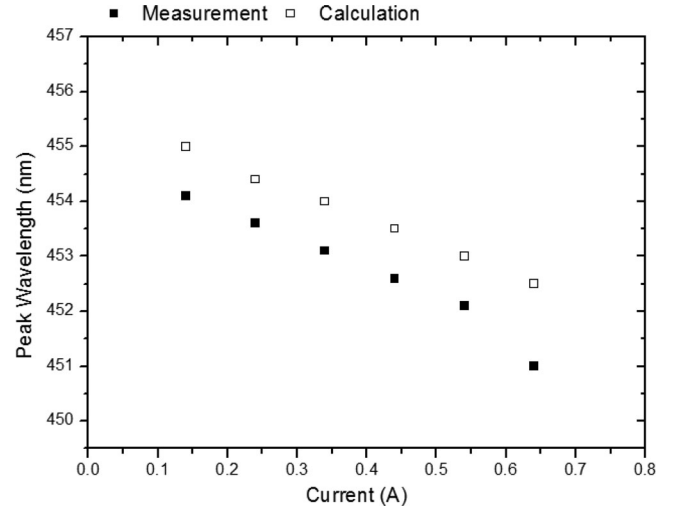
right-hand side of the equation are assumed to be constant. The second positive component $\left(\ln(\frac{I}{\beta})\frac{nkT_j}{h}\right)$ is a monotonically increasing function of junction temperature and current and the third negative component $\left(-\ln(T_j)\frac{2nkT_j}{h}\right)$ is a monotonically increasing function of the junction temperature.

The variation of the logarithmic contribution is significant at low injection current I range near zero, but becomes less dominant as the current becomes larger. In the initial low current range, the effect of an increasing current on the second term is larger than that of the thermal effect in the third term. As the current becomes larger, the thermal effect of the third term becomes more dominant in affecting the variation of the peak wavelength. Therefore, at low current level, the increase in the current will reduce the peak wavelength and upon reaching a minimum point, the peak wavelength will increase with the current. This means that the relationship of the peak wavelength and the LED current is of parabolic nature and has a minimum value. Such a relationship reflecting the true nature of LEDs was not considered in the works reported in [12]–[14].

III. SIMPLIFIED MODEL OF PEAK-WAVELENGTH SHIFT UNDER BILEVEL DRIVING

In this section, a simplified mathematical peak-wavelength-shift model will be derived for the case of LEDs driven by a bilevel current. By definition, a bilevel current is a PWM-like current that pulsates between a higher current level I_H and a lower nonzero current level I_L, with a duty cycle D representing the duration of I_H normalized to the pulse repetition time. Interested readers are referred to [13], which describes the original n-level driving and where the idea of using the bilevel current on LED originates from [19]. The average forward current I_{ave} and the peak wavelength of the LED at steady state can be, respectively, expressed as

$$I_{\mathrm{ave}} = DI_H + (1-D)I_L \tag{15}$$

and

$$v_p = \frac{c}{\lambda_p} = \begin{cases} D v_p(I_H, T_j) + (1 - D) v_p(I_L, T_j) & \text{for } I_L > 0 \\ v_p(I_H, T_j) & \text{for } I_L = 0. \end{cases}$$
(16)

According to (16), the peak frequency v_p approaches the values corresponding to I_H and I_L at large and small duty cycles, respectively, but is nonlinearly mixed within the intermediate duty cycles.

With a change in both D and T_j, the corresponding change in λ_p can be expressed as

$$d\left(\frac{c}{\lambda_p}\right) = [v_p(I_H) - v_p(I_L)]\,dD + D[dv_p(I_H) - dv_p(I_L)]$$

$$+ dv_p(I_L)$$

$$= [v_p(I_H) - v_p(I_L)]\,dD + D\left[\frac{d(v_p(I_H))}{d(T_j)}\right.$$

$$\left. - \frac{d(v_p(I_L))}{d(T_j)}\right]dT_j + \frac{d(v_p(I_L))}{d(T_j)}dT_j.$$
(17)

By considering the following assumption,

$$\frac{d(v_p(I_H))}{d(T_j)} = \frac{d(v_p(I_L))}{d(T_j)} = \frac{\partial v_p(I)}{\partial T_j}$$
(18)

(17), which gives the variation of λ_p with the change in D and T_j, can be simplified as

$$d\left(\frac{c}{\lambda_p}\right) = [v_p(I_H) - v_p(I_L)]\,dD + \frac{d(v_p(I_L))}{d(T_j)}dT_j.$$
(19)

The junction temperature T_j for an LED mounted on a heatsink under bilevel driving is

$$T_j = T_a + (R_{jc} + N R_{hs})[(I_H - I_L)k_h V_{ave}D + I_L V_{ave}k_h].$$
(20)

Next, differentiating T_j with respect to D gives

$$\frac{dT_j}{dD} = (R_{jc} + N R_{hs})(I_H - I_L)k_h V_{ave}.$$
(21)

By substituting (21) into (19), the variation of the peak wavelength on T_j can be expressed as

$$d\left(\frac{c}{\lambda_p}\right) = [v_p(I_H) - v_p(I_L)]$$

$$\times \frac{dT_j}{(R_{jc} + N R_{hs})(I_H - I_L)k_h V_{ave}} + \frac{d(v_p(I_L))}{d(T_j)}dT_j.$$
(22)

Putting (10) and (12) into (22) gives the expression for the variation of peak wavelength with respect to the change in T_j as

$$d\left(\frac{c}{\lambda_p}\right) = \left[\left(\ln\left(\frac{I_H}{I_L}\right)\frac{nk\left(D + \frac{I_L}{(I_H - I_L)}\right)}{h}\right)\right.$$

$$+ \ln\left(\frac{I_L}{\beta}\right)\frac{nk}{h} - \frac{2nk}{h}\Big(\ln[T_a + (R_{jc} + N R_{hs})$$

$$\left. \times (DI_H + (1 - D)I_L)k_h V_{ave}] - 1\Big)\right]dT_j.$$
(23)

Next, by substituting (21) into (22) and rearranging the equation with respect to the change in D, we have

$$d\left(\frac{c}{\lambda_p}\right) = \left([v_p(I_H) - v_p(I_L)] + \frac{d(v_p(I_L))}{d(T_j)}\frac{dT_j}{dD}\right)dD.$$
(24)

Putting (10), (12), and (21) into (24) gives the expression for the variation of peak wavelength with respect to the change in D as

$$d\left(\frac{c}{\lambda_p}\right) = \left(\left[\ln\left(\frac{I_H}{\beta}\right)\frac{nkT_j}{h} - \ln\left(\frac{I_L}{\beta}\right)\frac{nkT_j}{h}\right]\right.$$

$$+ \left(\ln\left(\frac{I_L}{\beta}\right)\frac{nk}{h} - \frac{2nk}{h}[\ln(T_j) - 1]\right)$$

$$\left. \times (R_{jc} + N R_{hs})(I_H - I_L)k_h V_{ave}\right)dD.$$
(25)

The corresponding minimum variation of the peak frequency $(dv_p)_{\min}$ with respect to the change in D and T_j is

$$(dv_p)_{\min} = \left(\left[\ln\left(\frac{I_H}{\beta}\right)\frac{nkT_j}{h} - \ln\left(\frac{I_L}{\beta}\right)\frac{nkT_j}{h}\right]\right.$$

$$+ \left[\ln\left(\frac{I_L}{\beta}\right)\frac{nk}{h} - \frac{2nk}{h}[\ln(T_j) - 1]\right]$$

$$\left. \times (R_{jc} + N R_{hs})(I_H - I_L)k_h V_{ave}\right) = 0.$$
(26)

If the peak frequency variation is reduced to the minimal, the relationship of the electrical, thermal, and physical parameters can be obtained by solving (26) to give

$$\frac{[\ln(I_H) - \ln(I_L)]I_{ave}}{I_H - I_L} =$$

$$\left\{2[\ln((R_{jc} + N R_{hs})k_{h\_ave}V_{ave}I_{ave}) - 1] - \ln\left(\frac{I_L}{\beta}\right)\right\}.$$
(27)

Notably, when the peak frequency variation is minimal, the peak wavelength variation should be minimal. Several important observations can be drawn from the equation.

1) Similar to the dc driving method, for bilevel driving, for the same average LED current the peak frequency-temperature sensitivity is higher with a lower heatsink thermal resistance. If a larger heatsink (i.e., lower R_{hs}) is used, the smaller the shift of the peak wavelength becomes.

2) For minimum variation of the peak frequency, the low-current level I_L should be lower than a certain value under a given thermal design. However, since the left term of (27), i.e., $\frac{[\ln(I_H) - \ln(I_L)]I_{ave}}{I_H - I_L}$, must be a positive value, $\ln(\frac{I_L}{\beta})$ should be smaller than $2[\ln((R_{jc} + N R_{hs})k_h V_{ave}I_{ave}) - 1]$.

3) To stabilize the variation of the peak frequency, I_L should be lower than a certain value depending on the heat dissipation coefficient k_h, thermal resistances of device R_{jc} and heatsink R_{hs}, and the physical parameter β.
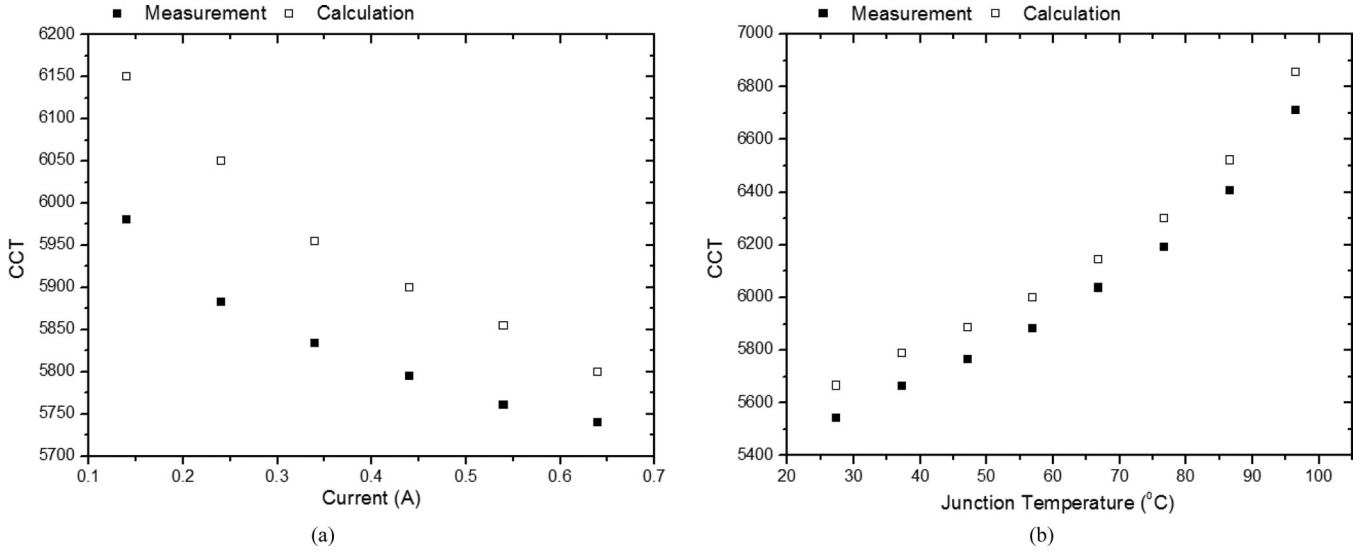
Fig. 3.   (a) CCT versus current at constant junction temperature of 56 °C ; (b) CCT versus junction temperature at constant current of 240 mA.

4) The term $\ln(I_H) - \ln(I_L)$ is negligible as compared to $I_H - I_L$. Therefore, for a given low current level I_L and average current I_{ave}, the minimum variation of the peak wavelength depends on the thermal resistance of heatsink. It is recommended that a larger value of high current level I_H be given for an LED mounted on a heatsink with low thermal resistance to minimize the peak-wavelength variation. A lower duty cycle D should be adopted to maintain a constant I_{ave} in this case.

5) For the same heatsink, the peak wavelength is more sensitive to temperature variation at a lower average current.

6) For a given set of current levels I_H and I_L, the variation of the peak wavelength depends on both the thermal resistance of heatsink R_{hs} and duty cycle D. If a higher thermal resistance of the heatsink is chosen, the duty cycle D should be decreased along with a lower average current I_{ave}.

According to (13) and (14), the variation of the peak wavelength is monotonous with the change of junction temperature and current, and this affects the phosphor emission efficiency, spectra, and thus the CCT. As shown in Fig. 3, which gives both the simulation and experimental results, the CCT decreases with a higher injection current at a constant junction temperature and increases with a higher junction temperature at a constant current.

For any given heatsink, the operating point I at which the minimum peak wavelength λ_p occurs can be determined. Conversely, known values of the operating characteristic of the LED system can be used for the selection of the heatsink. The parameters V_0, n, β, and ΔV_{el} are difficult to determine precisely as they depend on the die material and physical structure of the LED. These parameters can be found through a genetic algorithm (GA) search using measured results of the LED. With the measured peak wavelength and current, the GA algorithm used for finding the optimum solution is

$$J(n, V_0, C, \Delta V_{el}) = \min\left[\sum(\lambda_{p_i} - \lambda'_{p_i})^2 + (I_i - I'_i)^2\right] \quad (28)$$
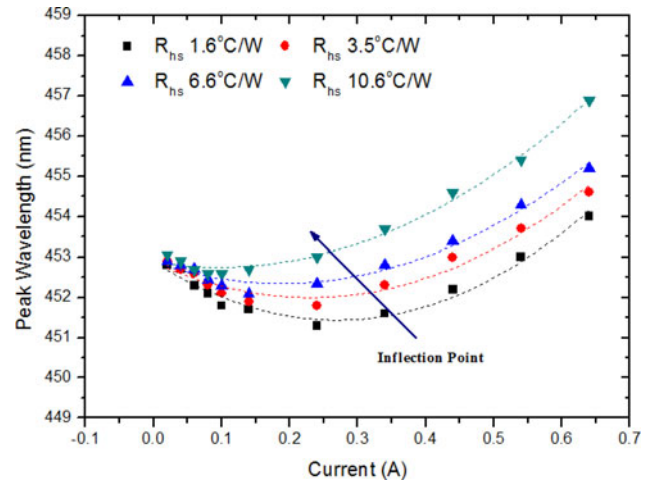
Fig. 4.   Measured peak wavelength with the current of the cool-white LED on different heatsinks under a dc drive.

where $J(n, V_0, C, \Delta V_{el})$ is the objective function, λ_{p_i} and λ'_{p_i} are the measured and calculated peak wavelengths, and I_i and I'_i are the measured and calculated currents. A set of $(V_0, n, C, \Delta V_{el})$ can be searched within a domain of potential solutions so that the function on the right-hand side of (28) is minimized. The validity of (10) for selecting a heatsink that can influence the changing trend of the peak wavelength under a dc drive is investigated. Respectively, Figs. 4 and 5 show the variations of the measured peak wavelength and CCT with the LED current for a range of heatsink thermal resistance. It can be seen that a small variation of the measured peak wavelength can lead to a large variation of the CCT due to the change in the spectral power distribution. As shown in (10), the change in current and heat can, respectively, cause a blue shift and a red shift to the peak wavelength.

The CCT function has a similar parabolic nature as the peak-wavelength function does (see Fig. 6), and therefore, there are two current points I_1 and I_2, which give the same $CCT_{\_12}$. These two points converge at the minimum $CCT_{\_0}$ when $I_1 = I_2 = I_0$.
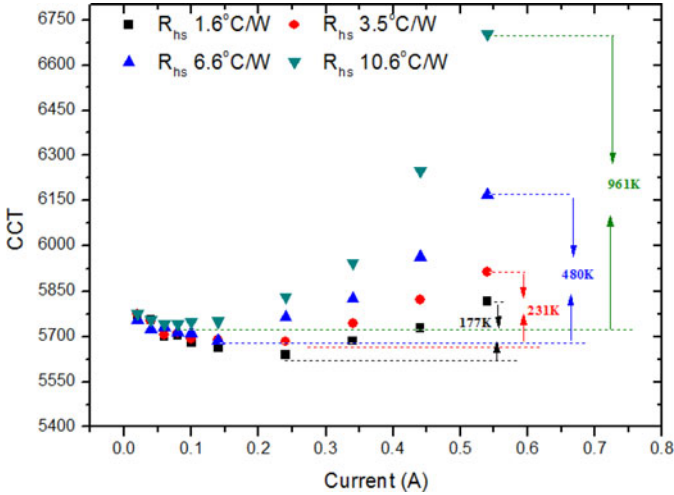
Fig. 5. Measured CCT with the current of the cool-white LED on different heatsinks under a dc drive.

As the current increases from I_0 to I_2, the effect of blue shift due to the change of the current gradually diminishes, while the influence of red shift due to the change of the junction temperature becomes increasingly dominant (as the temperatures increases to $CCT_{\_12}$). Conversely, as the current decreases from I_0 to I_1, the degree of the red shift gradually diminishes, while the blue shift becomes increasingly dominant (as color temperature increases to $CCT_{\_12}$).

Given a CCT function, a dimming range $(I_1 - I_2)$ can be selected to follow a CCT $(\Delta_{\max} - \Delta_{\min})$ profile as illustrated in Fig. 6(b). With an LED operating with a CCT curve that has a small gradient around the minimum CCT point, a relatively large dimming range with very small CCT variation (i.e., small sensitivity of the hue variation) is possible. The human sensitivity toward the CCT tolerance (i.e., variation) is different for a warm and a cool light source. Several important observations are drawn from Fig. 6 and the ANSI Standard C78.377 [22]:

1) for a warm-white LED (2700 K), if the CCT variation is limited to less than 145 K for the current range $I_1 - I_2$, the color variation will not be noticeable during the entire dimming process;
2) for a cool-white LED (5700 and 6500 K), if the CCT variation is limited to 355 and 510 K, respectively, over dimming, the color variation is not noticeable.

Referring back to Figs. 4 and 5, it is evident that for a heatsink's thermal resistance of 1.6 °C/W, the overall peak wavelength of cool-white LEDs under a dc drive is almost constant with little variation (< 2 nm) for the current between 0.074 and 0.54 A. For the same heatsink, the CCT variation of cool-white LED is within 177 K when the dimming current changes from 0.08 to 0.54 A (i.e., a dimming range of 0.46 A). Note that with a heatsink's thermal resistance of 1.6 °C/W, the color variation of the cool-white LED under the full dimming range is obviously not noticeable. With the thermal resistance increased to 3.5 °C/W, the CCT variation is increased to within 231 K for the same current range, which is still below the perceptible CCT limit of 355 K. However, if the thermal resistance is increased

to 6.6 °C/W, the CCT variation will be significantly increased to 480 K, which exceeds the limit. To ensure that the CCT variation is kept within the acceptable limit, the operating current range can be reduced to range of 0.08 to 0.44 A. Clearly, a smaller thermal resistance of the heatsink leads to a larger dimming current range with a minimal change of the peak wavelength and CCT.

IV. CCT SHIFT REDUCTION METHODS BASED ON BILEVEL AND DC DRIVES

A. CCT Shift Reduction Under Steady State

As discussed, the choice of a suitable dimming range could effectively reduce the overall CCT variation. The optimal operating range in terms of hue can be selected simply by choosing the current range and a suitable heatsink. To further reduce the CCT variation, the control of the heatsink temperature through active means can be adopted. For example, further color-shift reduction can be accomplished dynamically by an adaptive change of the junction temperature with a temperature-controlled heatsink.

1) Under a DC Drive: Fig. 7 shows the measured CCT points of an LED under the dc drive, of which the CCT is kept within limit through the reduction of the heatsink temperature. The permissible range of controllable temperature for the LED with a heatsink of thermal resistance of 10.6 °C/W is wider than that of thermal resistance of 1.6 °C/W. For a given current, the temperature sensitivity of the peak wavelength depends on the thermal resistance of the heatsink. Therefore, for the same current, the peak frequency–temperature sensitivity of an LED mounted on a smaller heatsink with a higher R_{hs} will be higher. For a current of 0.64 A, Fig. 7(a) shows that the temperature of a heatsink with a thermal resistance of 1.6 °C/W has to be reduced by 18.0 °C, in order to adjust the CCT to the minimum value of the parabolic curve. But for a heatsink with a large thermal resistance of 10.6 °C/W, its temperature has to be reduced by 61.0 °C for the same minimum CCT value.

Note that with the thermal resistance of 1.6 °C/W, the amplitude shift of the CCT is very small within the optimized range. This implies the following:

1) if the thermal design is not restricted by space, a big heatsink with low R_{hs} should always be selected for the LED system in order to effectively reduce the overall CCT variation;
2) with an active temperature control, an LED system with a lower R_{hs} requires less thermal energy for controlling and stabilizing the CCT than that with a higher R_{hs}.

As illustrated in Fig. 8, if the LED is driven by a dc current, the light output of the LED will reach a maximum level at a certain current, and then decreases as the current increases. The control of light output using the dc drive current is achieved by adjusting the forward current flowing through the LED via a current sensing and voltage feedback-control mechanism. In the case of bilevel driving (or n-level driving), a lower current $I_{\min}$ is applied to the LED for a time period t_{OFF} to produce a luminous flux $\Phi_{v\_\min}$, and then followed by a higher current $I_{\max}$ for a time period t_{ON} to produce a luminous flux of $\Phi_{v\_\max}$. The actions are repeated periodically. Thus, the average
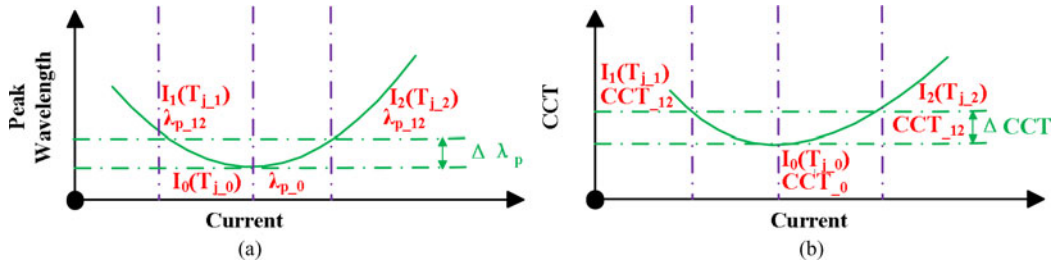
Fig. 6. (a) Example of reducing peak wavelength variation using the bottom region of the peak wavelength curve ; (b) example of reducing CCT variation using the bottom region of the CCT.

(a)

(b)
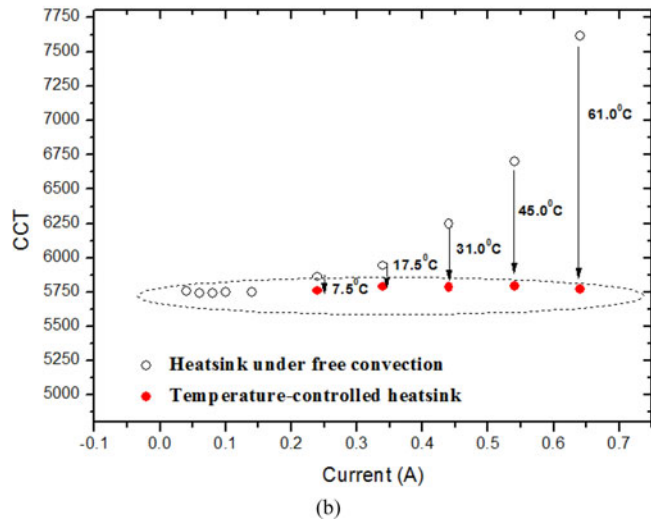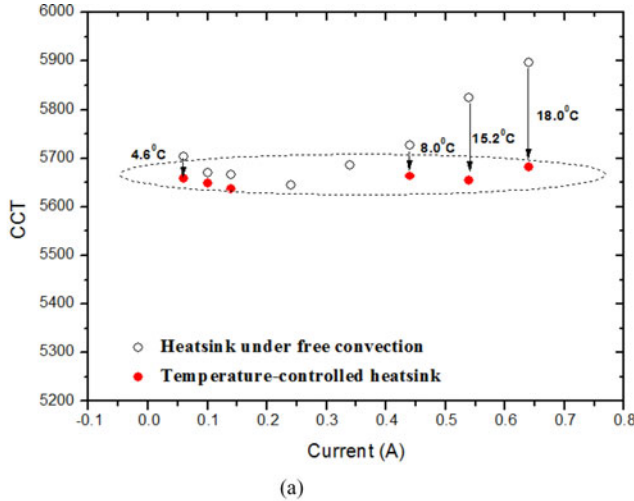
Fig. 7. Measured CCT of an LED under a dc drive with and without heatsink temperature control. Heatsink thermal resistance of (a) 1.6 °C/W and (b) 10.6 °C/W.

luminous flux is a linear function given by $\Phi_{v\_ave} = D\Phi_{v\_max} + (1-D)\Phi_{v\_min}$ which corresponds to the average applied current described in (15). Thus, the light output is controlled by adjusting the duty cycle, which can be more precise than the adjustment of the current level.

2) Under a Bilevel Drive: A comparison of the luminous flux curve of the dc drive and bilevel drive shows that the flux difference $\Delta\Phi_v$ between the bilevel and dc drives with
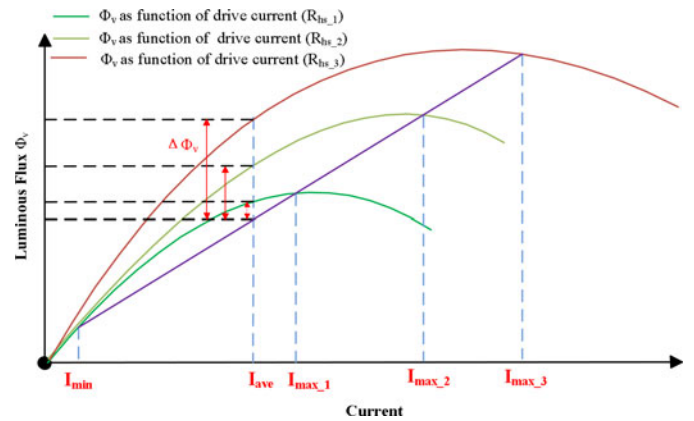
Fig. 8. Typical luminous flux characteristic of LED under dc and bilevel current drive with different heatsinks.

the same average current decreases when the thermal resistance of heatsink is smaller because the duty cycle average of the bilevel drive is dominated by the higher current I_{max}, which has a lower energy-efficiency operating point. In general, the electrical power of the LED comprises two portions, namely, the optical power portion and the heat portion (defined as k_h which is the ratio of heat power over the total electrical power). From the previous analysis, two points should be noted:

1) for any given electrical power, k_h of the LED under a bilevel drive is higher than that of a dc drive, leading to a higher junction temperature;
2) with a lower R_{hs}, the difference in the range of k_h between the bilevel and the dc drive is wider and should be reduced.

As shown in Fig. 9, the CCT variation of an LED can be reduced by controlling the heatsink temperature under a bilevel drive. For an average current of 0.54 A, in order to adjust the CCT to the minimum value (i.e., the inflection point of parabolic curve), the temperature of the heatsink with a thermal resistance of 1.6 °C/W should be decreased by 23.0 °C [Fig. 9(a)]. But for a heatsink with thermal resistance of 10.6 °C/W, its temperature should be decreased by 56.0 °C [Fig. 9(b)].

Two important points to note are as follows:

1) for a given current and heatsink, the peak wavelength–temperature sensitivity of the LED under a dc drive is lower than that under a bilevel drive, as reflected in Figs. 7 and 9;

for example, for a current of 0.54 A and a thermal resistance of 1.6 °C/W, in order to reach the same minimum
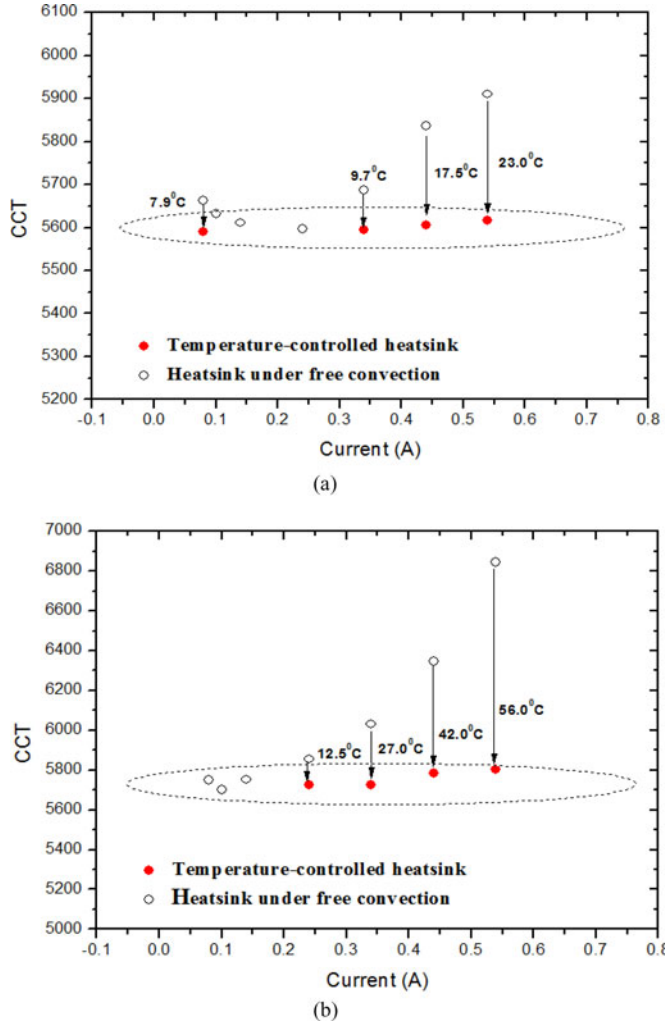
Fig. 9. Measured CCT of an LED under a bilevel drive (I_{high} = 0.64 A, I_{low} = 0.04 A) for a heatsink of thermal resistance (a) 1.6 °C/W and (b) 10.6 °C/W, with and without temperature control.

point of the CCT, the temperature of the LED under a dc drive is decreased by 15.2 °C and that of bilevel drive is decreased by 23.0 °C;

2) an LED under a dc drive requires less thermal energy to achieve its CCT stabilization than that under the bilevel drive.

B. CCT Shift Reduction Under Dynamic State

Fig. 10 shows the dc-driven curve and three sets of bilevel driven curves with the same average current for an LED mounted on heatsinks with low [Fig. 10(a)] and high [Fig. 10(b)] thermal resistance. The flux difference $\Delta\Phi_{\_12}$ and temperature difference ΔT_{j_12} between different bilevel current pair amplitudes with the same average current (constant duty cycle) increase when the thermal resistance of heatsink increases because the device operates at a higher current I_{high} which has a lower energy-efficiency operating point (higher k_h and junction temperature).

The measured CCT versus current curve is of a similar parabolic nature to the theoretical function and, therefore, there are two current points I_{low} and I_{high} which give the same CCT

in the dc driving method. Due to the dynamic switching actions of the bilevel driving method, its CCT variation function will be different from that of the dc driving method, as shown in Fig. 11(a) and (b). As the junction temperatures resulting from $I_{\text{low\_Bi(1)}}$ and $I_{\text{high\_Bi(1)}}$ in the bilevel driving method are, respectively, higher and lower than that of $I_{\text{low\_dc}}(T_{j\_l})$ and $I_{\text{high\_dc}}(T_{j\_h})$ in the dc driving method, the CCT of the former will be, respectively, higher and lower than that of the latter. While the current injected into the device has two amplitudes ($I_{\text{low\_Bi}}$ and $I_{\text{high\_Bi}}$) in the bilevel drive, the average current ($I_{\text{ave\_Bi(1)}}$ and $I_{\text{ave\_Bi(2)}}$) is still dependent on the duty cycle.

Several points should be noted:
1) the variation trend for CCT versus current is dependent not only on the average current of the bilevel driving method, but also on the junction temperature;
2) for a given constant average current, the CCT variation is dependent on the bilevel current amplitude. As shown in Fig 11(a), with a constant average current of $I_{\text{ave\_Bi(1)}}$, if the current amplitude of $I_{\text{low\_Bi(1)}}$ is lower than that of $I_{\text{low\_Bi(1\_2)}}$, the junction temperature of $I_{\text{low\_Bi(1)}}$ will be higher than that of $I_{\text{low\_Bi(1_2)}}$ due to nonlinear relationship of the luminous flux–current, as shown in Fig 10(a);
3) the inflection region of the CCT variation curve is dependent on the thermal resistance of the heatsink.

The CCT dynamic performance of the LED under the bilevel drive is explored using a low and high current that is set with a constant duty cycle of $D = 0.5$ and changing at a frequency of 1 Hz. Fig. 11(c) shows the measured CCT variation of the LED under the 1-Hz bilevel drive for a different heatsink thermal resistance of 1.6 °C/W and 10.6 °C/W under thermal equilibrium. With a thermal resistance of 1.6 °C/W, the CCT variation is about 176 K with the current switching between I_{high} = 0.342 A and I_{low} = 0.04 A. It could be reduced to 45 K if I_{high} = 0.51 A and I_{low} = 0.12 A. If the thermal resistance increases to 10.6 °C/W, the CCT variation is about 213 K with the current switching between I_{high} = 0.592 A and I_{low} = 0.172 A, and is reduced to 42 K if I_{high} = 0.466 A and I_{low} = 0.165 A.

From the results, the following observations are noted:
1) CCT is not constant between the high and low currents. However, the overall CCT variation can be significantly reduced with a proper choice of dimming current range and it could be kept small over the full dimming range;
2) a smaller dimming current range does not necessarily lead to a smaller CCT change (since the dimming current range cuts across the inflection point of the parabolic curve given in Fig. 6);
3) if the thermal design is constricted by space such that the inflection point of the CCT variation curve occurs at a lower power, then the LED system should be designed to operate with a narrow dimming range.

V. CONCLUSION

The color-shift properties of white LEDs under the dc and bilevel drives are discussed using a simplified peak-wavelength model proposed in this paper. This model is based on a simple transitional photon energy model for LED and can be used to predict the inflection point of peak wavelength variation.
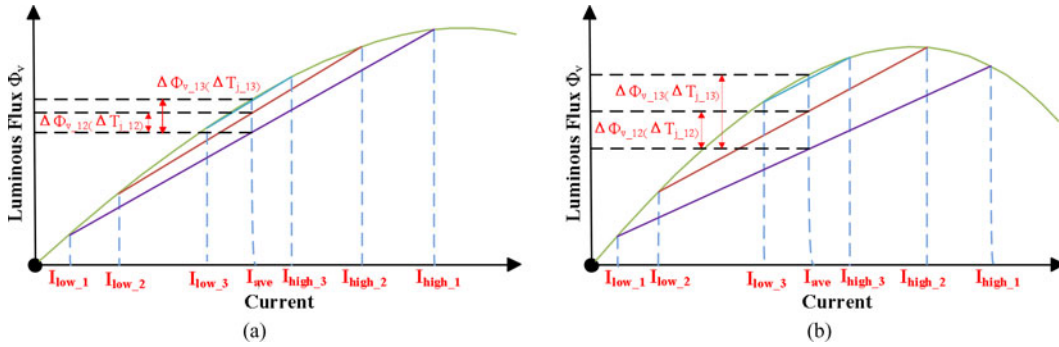
Fig. 10.   Typical characteristics of luminous flux of LED under dc and bilevel current drive with different heatsinks of (a) low thermal resistance and (b) high thermal resistance.
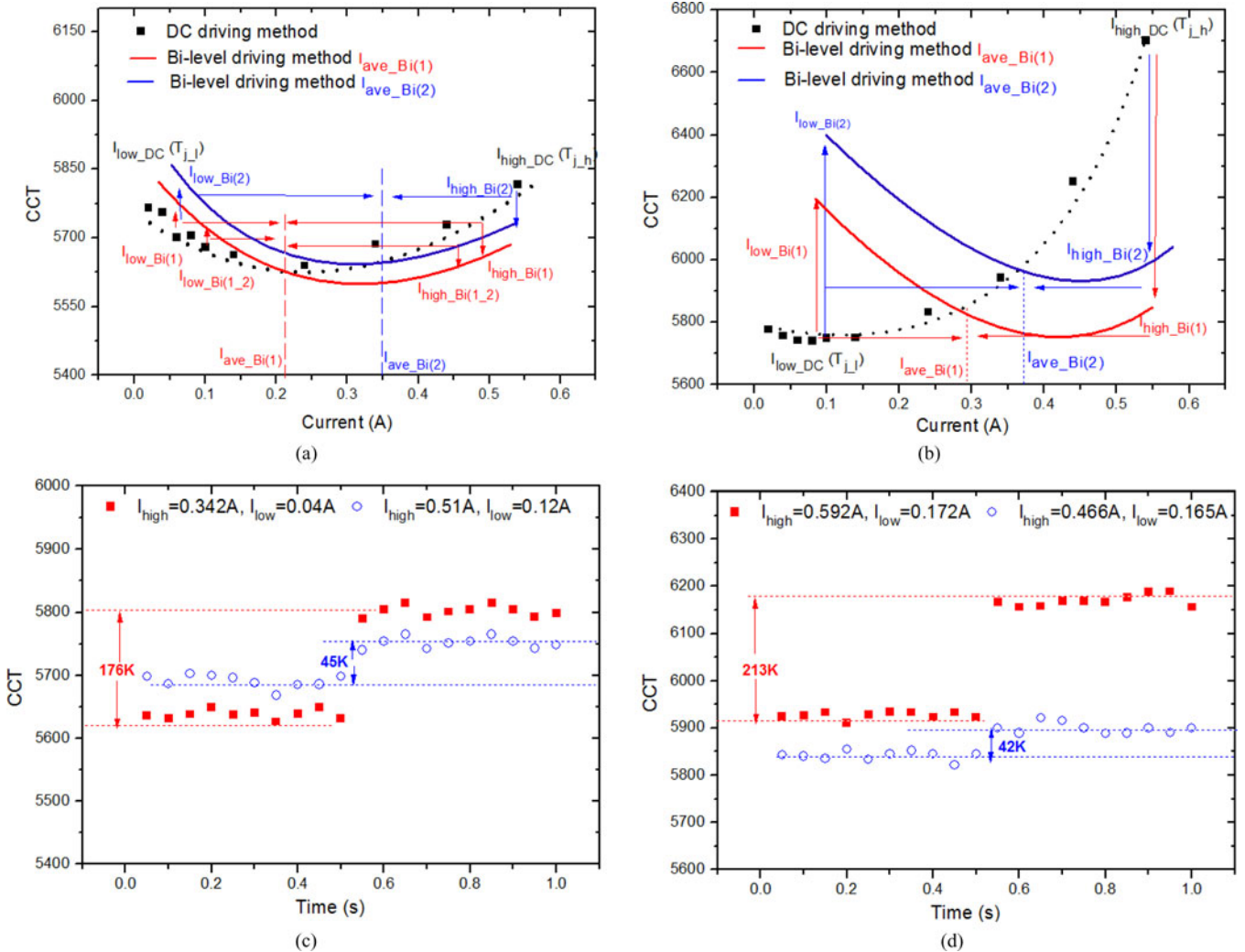
Fig. 11.   Measured CCT versus current of cool-white LEDs under dc driving and bilevel driving methods with constant duty cycle and average current with heatsinks of thermal resistance of (a) 1.6 °C/W and (b) 10.6 °C/W. Measured CCT of LEDs under a 1-Hz bilevel driving method with heatsinks of thermal resistance of (c) 1.6 °C/W and (d) 10.6 °C/W.

Analytical study shows that the variation of the drive current and junction temperature have opposing effects on the changes of the peak wavelength and therefore the CCT. It is emphasized that the CCT of the LED is a complex relationship between the drive current level, duty cycle, thermal resistance, heat dissipation conversion ratio, and the physical parameters of the LED device. It is found that, for a given thermal design, reduction in CCT variation of an LED over a dimming range is possible by adjusting the combination of the current levels and the duty cycle. Reduction of CCT variation over a dimming range under both steady and dynamic states has been practically achieved. The proposed method can be easily adopted for improving the

CCT stabilization of the white LED systems. The results also show that an LED system under a dc drive requires less thermal energy for stabilizing the CCT than that under a bilevel drive.

REFERENCES

[1] J. Garcia, M. A. Dalla-Costa, J. Cardesin, J. M. Alonso, and M. Rico-Secades, "Dimming of high-brightness LEDs by means of luminous flux thermal estimation," *IEEE Trans. Power Electron.*, vol. 24, no. 4, pp. 1107–1114, Apr. 2009.

[2] M. Dyble, N. Narendran, A. Bierman, and T. Klein, "Impact of dimming white LEDs: Chromaticity shifts due to different dimming methods," *Proc. SPIE*, vol. 5941, pp. 291–299, Sep. 2005.

[3] S. Y. R. Hui and Y. X. Qin, "A general photo-electro-thermal theory for light-emitting-diode (LED) systems," *IEEE Trans. Power. Electron.*, vol. 24, no. 8, pp. 1967–1976, Aug. 2009.

[4] S. Y. R. Hui, "Methods for optimal operation of light emitting diodes," U.S. Patent 12/370101 13, Feb. 2009.

[5] S. Y. R. Hui, H. T. Chen, and X. H. Tao, "An extended photoelectrothermal theory for LED systems—A tutorial from device characteristic to system design for general lighting *(Invited Paper)*," *IEEE Trans. Power. Electron.*, vol. 27, no. 1, pp. 4571–4583, Nov. 2012.

[6] M. Leroux, N. Grandjean, M. Laugt, J. Massies, B. Gil, P. Lefebvre, and P. Bigenwald, "Quantum confined stark effect due to built-in internal polarization fields in (Al,Ga)N/GaN quantum wells," *Phys. Rev. B*, vol. 58, no. 20, pp. R13371–R13374, Nov. 1998.

[7] V. P. Varshni, "Temperature dependence of the energy gap in semiconductors," *Physica*, vol. 34, no. 1, pp. 149–154, Apr. 1967.

[8] N. Narendran, N. Maliyagoda, L. Deng, and R. Pysar, "Characterizing in LEDs for general illumination applications: Mixed-color and phosphor-based white sources," *Proc. SPIE*, vol. 4445, pp. 137–147, Jul. 2001.

[9] F. C. Wang, C. W. Tang, and B. J. Huang, "Multivariable robust control for a red-green-blue LED lighting system," *IEEE Trans. Power Electron.*, vol. 25, no. 2, pp. 417–428, Feb. 2010.

[10] H. K. Fu, C. W. Lin, T. T. Chen, C. L. Chen, P. T. Chou, and C. J. Sun, "Investigation of dynamic color deviation mechanisms of high power light-emitting diode," *Microelectron. Rel.*, vol. 52, pp. 866–871, May 2012.

[11] Y. Gu, N. Narendran, T. Dong, and H. Wu, "Spectral and luminous efficacy change of high-power LEDs under different dimming methods," *Proc. SPIE*, vol. 6337, pp. 63370J1–63370J7, Aug. 2006.

[12] K. H. Loo, Y. M. Lai, S. C. Tan, and C. K. Tse, "On the color stability of phosphor-converted white LEDs under dc, PWM, and bi-level drive," *IEEE Trans. Power. Electron.*, vol. 27, no. 2, pp. 974–984, Feb. 2012.

[13] S. C. Tan, "General *n*-level driving approach for improving electrical-to-optical energy-conversion efficiency of fast-response saturable lighting devices," *IEEE Trans. Ind. Electron.*, vol. 57, no. 4, pp. 1342–1353, Apr. 2010.

[14] K. H. Loo, Y. M. Lai, S. C. Tan, and C. K. Tse, "Stationary and adaptive color-shift reduction methods based on the bi-level driving technique for phosphor-converted white LEDs," *IEEE Trans. Power Electron.*, vol. 26, no. 7, pp. 1943–1953, Jul. 2011.

[15] E. F. Schubert, *Light-Emitting Diodes*, 2nd ed. Cambridge, London, U. K.: Cambridge Univ. Press, 2006.

[16] Y. J. Lee, C. J. Lee, and C. H. Chen, "Determination of junction temperature in InGaN and AlGaInP light-emitting diodes," *IEEE J. Quantum Electron.*, vol. 46, no. 10, pp. 1450–1455, Oct. 2010.

[17] S. K. Cheung and N. W. Cheung, "Extraction of Schottky diode parameters from forward current–voltage characteristics," *Appl. Phys. Lett.*, vol. 49, no. 2, pp. 85–87, Jul. 1986.

[18] D. Zhu, J. Xu, A. N. Noemaun, J. K. Kim, E. F. Schubert, M. H. Crawford, and D. D. Koleske, "The origin of the high diode-ideality factors in GaInN/GaN multiple quantum well light-emitting diodes," *Appl. Phys. Lett.*, vol. 94, no. 8, pp. 081113-1–081113-3, Feb. 2009.

[19] W. K. Lun, K. H. Loo, S. C. Tan, Y. M. Lai, and C. K. Tse, "Bi-level current driving technique for LEDs," *IEEE Trans. Power Electron.*, vol. 24, no. 12, pp. 2920–2932, Dec. 2009.

[20] A. Poppe, G. Farkas, V. Székely, G. Horváth, and M. Rencz, "Multi-domain simulation and measurement of power LED-s and power LED assemblies," in *Proc. IEEE 22nd Semicond. Thermal Meas. Manag. Symp.*, Mar. 2006, pp. 191–198.

[21] G. Farkas, Q. V. V. Vader, A. Poppe, and G. Bognár, "Thermal investigation of high power optical devices by transient testing," *IEEE Trans. Compon. Packag. Technol.*, vol. 28, no. 1, pp. 45–50, Mar. 2005.

[22] *Specifications for Chromaticity of Solid State Lighting Products*, ANSI Standard C78.377, 2008.

Huan-Ting Chen (M'13) received the Ph.D. degree in radio physics from Xiamen University, Xiamen, China, in 2010. As a joint-program Ph.D. student, he studied in the Light and Lighting Laboratory, Catholic University College Ghent, Ghent, Belgium, from November 2009 to May 2010.

He was a Senior Research Associate in the Department of Electronic Engineering, City University of Hong Kong, Kowloon, Hong Kong, in 2011. He is currently a Postdoctoral Fellow in the Department of Electrical and Electronic Engineering, The University of Hong Kong, Hong Kong. His research interests include solid-state lighting theory and technologies.

Siew-Chong Tan (S'00–M'06–SM'11) received the B.Eng. (Hons.) and M.Eng. degrees in electrical and computer engineering from the National University of Singapore, Singapore, in 2000 and 2002, respectively, and the Ph.D. degree in electronic and information engineering from the Hong Kong Polytechnic University, Hung Hom, Hong Kong, in 2005.

From October 2005 to May 2012, he worked as a Research Associate, Postdoctoral Fellow, Lecturer, and Assistant Professor in the Department of Electronic and Information Engineering, Hong Kong Polytechnic University. From January to October 2011, he was a Senior Scientist in Agency for Science, Technology, and Research (A∗Star), Singapore. He is currently an Associate Professor in the Department of Electrical and Electronic Engineering, The University of Hong Kong, Hong Kong. He was a Visiting Scholar at Grainger Center for Electric Machinery and Electromechanics, University of Illinois at Urbana-Champaign, Champaign, IL, USA, from September to October 2009, and an Invited Academic Visitor of Huazhong University of Science and Technology, Wuhan, China, in December 2011. His research interests include power electronics and control, LED lightings, smart grids, and, clean energy technologies.

Dr. Tan serves extensively as a reviewer for various IEEE/IET TRANSACTIONS AND *Journals on Power, Electronics, Circuits, and Control Engineering*. He is a coauthor of the book *Sliding Mode Control of Switching Power Converters: Techniques and Implementation* (Boca Raton, FL, USA: CRC Press, 2011).
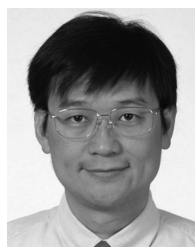
S. Y. (Ron) Hui (M'87–SM'94–F'03) received the B.Sc. (Hons.) degree in engineering from the University of Birmingham, Birmingham, West Midlands, U.K., in 1984 and the D.I.C. and Ph.D. degrees from Imperial College London, London, U.K., in 1987.

He has previously held academic positions at the University of Nottingham (1987–1990), University of Technology Sydney (1991–1992), University of Sydney (1992–1996), City University of Hong Kong (1996–2011). From July 2011, he holds the Chair Professorship at the University of Hong Kong. Since July 2010, he concurrently holds the Chair Professorship at Imperial College London.

Dr. Hui has published more than 200 technical papers, including more than 150 referred journal publications and book chapters. More than 50 of his patents have been adopted by industry. He is a Fellow of the IET. He has been an Associate Editor of the IEEE TRANSACTIONS ON POWER ELECTRONICS since 1997, and an Associate Editor of the IEEE TRANSACTIONS ON INDUSTRIAL ELECTRONICS since 2007. He has been appointed twice as an IEEE Distinguished Lecturer by the IEEE Power Electronics Society in 2004 and 2006. He served as one of the 18 Administrative Committee members of the IEEE Power Electronics Society and was the Chairman of its Constitution and Bylaws Committee from 2002 to 2010. He received the Excellent Teaching Award at CityU in 1998 and the Earth Champion Award in 2008. He won an IEEE Best Paper Award from the IEEEIAS Committee on Production and Applications of Light in 2002, and two IEEE Power Electronics Transactions Prize Paper Awards for his publications on Wireless Charging Platform Technology in 2009 and on LED system theory in 2010. His inventions on wireless charging platform technology underpin the key dimensions of Qi, the world's first wireless power standard, with freedom of positioning and localized charging features for wireless charging of consumer electronics. In November 2010, he received the IEEE Rudolf Chope R&D Award from the IEEE Industrial Electronics Society, the IET Achievement Medal (The Crompton Medal) and was elected for the Fellowship of the Australian Academy of Technological Sciences and Engineering.